A mathematical formulation of accelerating moment release based on the stress accumulation model

A Mignan, Geoffrey C.P. King, D Bowman

A mathematical formulation of accelerating moment release based on the stress accumulation model

A. Mignan,[1,2] G. C. P. King,[2] and D. Bowman[3]

Received 2 August 2006; revised 18 December 2006; accepted 16 April 2007; published 10 July 2007.

[1] Large earthquakes can be preceded by a period of accelerating seismic activity of moderate-sized earthquakes. This phenomenon, usually termed accelerating moment release, has yet to be clearly understood. A new mathematical formulation of accelerating moment release is obtained from simple stress transfer considerations, following the recently proposed stress accumulation model. This model, based on the concept of elastic rebound, simulates accelerating seismicity from theoretical stress changes during an idealized seismic cycle. In this view, accelerating moment release is simply the consequence of the decrease, due to loading, of the size of a stress shadow due to a previous earthquake. We show that a power law time-to-failure equation can be expressed as a function of the loading rate on the fault that is going to rupture. We also show that the m value, which is the power law exponent, can be defined as $m = D/3$, with D a parameter that takes into account the geometrical shape of the stress lobes and the distribution of active faults. In the stress accumulation model, the power law is not due to critical processes.

Citation: Mignan, A., G. C. P. King, and D. Bowman (2007), A mathematical formulation of accelerating moment release based on the stress accumulation model, *J. Geophys. Res.*, *112*, B07308, doi:10.1029/2006JB004671.

1. Introduction

[2] Accelerating moment release has been identified for a substantial number of earthquakes and observed for years to tens of years before a main shock over tens to hundreds of kilometers from the future epicenter [e.g., *Sykes and Jaumé*, 1990; *Bufe and Varnes*, 1993; *Knopoff et al.*, 1996; *Bowman et al.*, 1998; *Brehm and Braile*, 1998; *Jaumé and Sykes*, 1999; *Robinson*, 2000; *Bowman and King*, 2001; *Zoller et al.*, 2001; *Papazachos et al.*, 2002; *Bowman and Sammis*, 2004]. Although accelerating moment release might be fitted by any power law, it is typically modeled by a simple power law time-to-failure equation, following *Bufe and Varnes* [1993]. This is a relation of the form

$$\epsilon(t) = A + B(t_f - t)^m \tag{1}$$

where t_f is the time of the large event, B is negative and m is usually about 0.3. A is the value of $\epsilon(t)$ when $t = t_f$. For a convenient data analysis, $\epsilon(t)$ is chosen to be the cumulative Benioff strain at time t and is defined as

$$\epsilon(t) = \sum_{i=1}^{N(t)} \sqrt{E_i(t)} \tag{2}$$

where E_i is the energy of the ith event and $N(t)$ is the number of events at time t. The cumulative Benioff strain is preferred over the cumulative number of earthquakes because the multitude of smaller earthquakes would dominate the data, whereas the moderate to large events would dominate if the cumulative seismic energy alone was used. Therefore the choice of equation (2) has no physical meaning and is only an observational tool. In this work, we keep the term "accelerating moment release" as it is referred in numerous publications. Equation (1) is equivalent to the rate-dependent failure equation of *Voight* [1989] as noted by *Bufe and Varnes* [1993], but the physical relation of this expression to accelerating moment release is not verified, and other power laws based on different physical processes can fit the preevent seismicity rate changes.

[3] Since accelerating seismic activity is a promising tool for earthquake forecasting, it is important to determine the origin of accelerating moment release. The majority of studies consider that accelerating moment release is due to critical processes (i.e., self-organized criticality or critical point theory). Studies which give an explanation to the power law behavior of accelerating moment release are based on different critical concepts, such as the epidemic-type aftershock sequence model [e.g., *Sornette and Helmstetter*, 2002], the renormalization group theory for hierarchical systems [e.g., *Sornette and Sammis*, 1995; *Saleur et al.*, 1996], fiber-bundle models [e.g., *Newman and Phoenix*, 2001; *Turcotte et al.*, 2003], continuum damage mechanics [e.g., *Ben-Zion and Lyakhovsky*, 2002] or percolation models [e.g., *Sammis and Sornette*, 2002].

[4] The stress accumulation model recently proposed by *King and Bowman* [2003] also explains accelerating

[1]Risk Management Solutions, London, UK.
[2]Laboratoire Tectonique, Institut de Physique du Globe de Paris, Paris, France.
[3]Department of Geological Sciences, California State University, Fullerton, California, USA.

0148-0227/07/2006JB004671$09.00

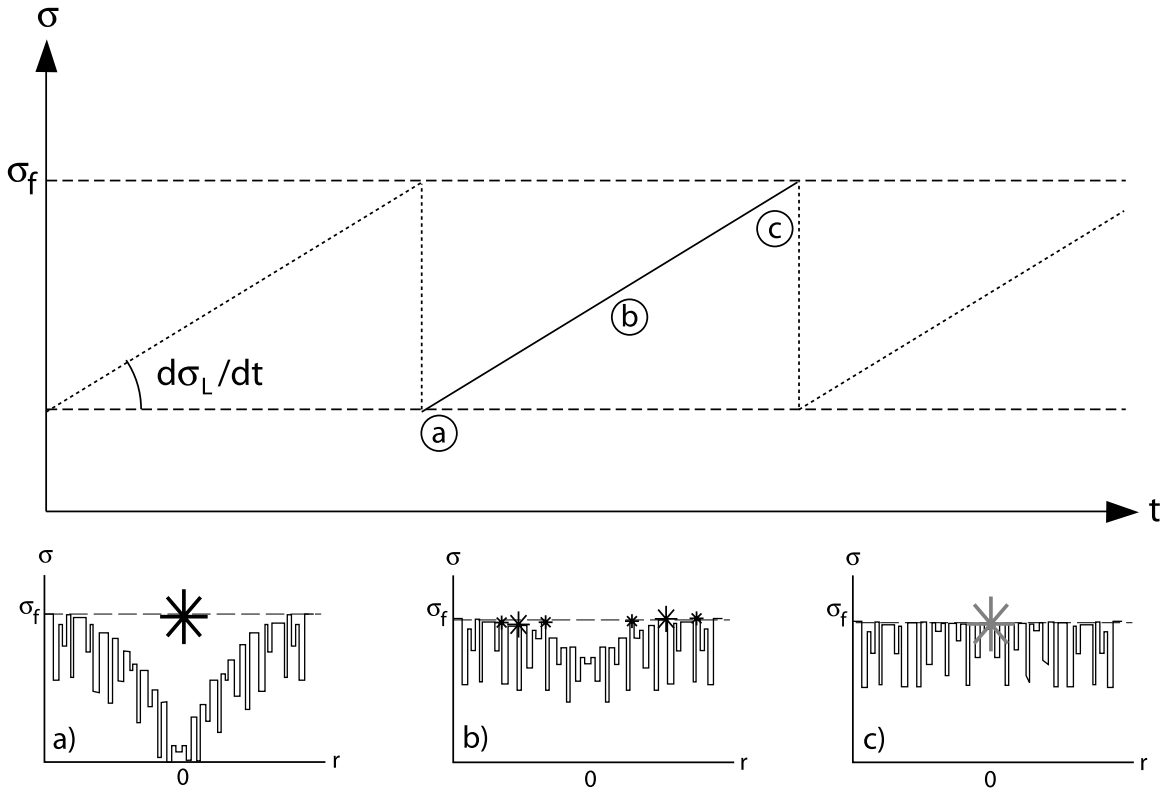

Figure 1. Schematic representation of the spatiotemporal evolution of regional seismicity, at the origin of accelerating moment release, during the seismic cycle of a given fault. (top) The loading rate $d\sigma_l/dt$ is constant on the fault and main shocks are periodic with a constant stress drop. (bottom) A background stress noise is added to simulate the background seismicity in space and time: (a) stress shadow after the main shock; (b) decrease of the size of the stress shadow; and (c) stress shadow completely filled prior to the next main shock. Large stars represent main shocks, and small black stars represent pre–main shock seismicity. Preevents occur when the stress σ exceeds the failure stress σ_f. Modified from *King and Bowman* [2003].

moment release. In this model, accelerating moment release is due to the decrease of the size of a stress shadow left from one or more previous events. Consequently the main cause of increasing seismicity is loading by creep at depth on the fault that is going to fail. This view is not the same as other explanations based on critical processes where the acceleration is due to cascade triggering. Moreover, *Mignan et al.* [2006b] showed that the spatial distribution of accelerating moment release is in agreement with the predictions of the Stress Accumulation but not with stress triggering. The purpose of this work is to determine a mathematical formulation in agreement with equation (1) based on the principles of the stress accumulation model, which could lead to a better understanding of how to use accelerating moment release for forecasting.

2. Mathematical Formulation

[5] In the stress accumulation model [*King and Bowman*, 2003], events occur at a constant rate (background seismicity) outside the stress shadow formed by the last main shock. In the simplest form of the model, the stress is not sufficient for failure in the stress shadow and corresponds to a region of quiescence. The central point of the model is that aseismic slip on the fault at depth loads the upper part of the crust slowly removing the stress shadow prior to the next major event (Figure 1). *King and Bowman* [2003] add a stress noise to the stress associated to the seismic cycle to simulate background seismicity. A new event occurs when the stress σ exceeds the failure stress σ_f.

2.1. Spatiotemporal Evolution of a Stress Shadow

[6] Let us consider the spatiotemporal evolution at the surface of a stress shadow during the seismic cycle of a theoretical fault (simplified to a point source at a given depth).

[7] The time evolution of the stress σ at $r = 0$ (epicenter) is

$$\sigma(r=0,t) = \sigma_0 + \frac{d\sigma_l}{dt}t \quad , \quad \sigma_0 = \sigma(r=0,t=0) \qquad (3)$$

where σ_0 is the stress drop from the last main shock (<0, value at the surface), $d\sigma_l/dt$ is the loading rate and t is the time from the last main shock. The loading rate is considered constant (Figure 1) on a fault in a purely elastic medium. This idealized fault is localized and extends through both the crust and upper mantle, which are both assumed to retain long-term strength. Over the timescale of the seismic cycle, changes of the loading rate due to viscous

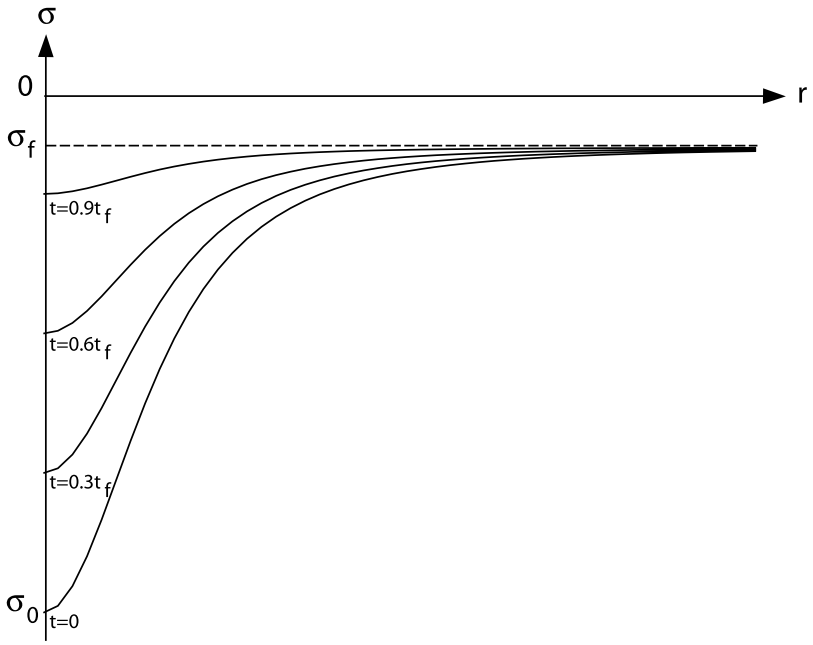

Figure 2. Evolution at the surface of the stress shadow ($\sigma < 0$) as a function of the distance from the source point (i.e., epicenter) for different times t to the final time t_f: $t = 0$, $t = 0.3\ t_f$, $t = 0.6\ t_f$, and $t = 0.9\ t_f$. Far from the stress shadow, the background stress is constant and tends to the failure stress σ_f. Note that except close to the source, the evolution is the same at any depth that is small compared to r.

relaxation in the lower crust or mantle are not required by either geological or recent geodetic data (see discussion by *King and Bowman* [2003]). Other processes such as time-dependent fault healing are not taken into account. Possible changes of the loading rate following a major earthquake are considered negligible since only precursory seismicity to the next major earthquake is studied.

[8] The spatial evolution of the stress σ from the epicenter to r is given as

$$\sigma(r) = B + \frac{A}{(r^2 + h^2)^{3/2}} \tag{4}$$

where h is the depth of the point source and A and B are defined using limit conditions. Equation (4) is obtained from the simple relation

$$\sigma(R) \propto \frac{1}{R^3} \tag{5}$$

where $R = \sqrt{r^2 + h^2}$. Although equation (5) is an oversimplification, it permits a dimensional study of the evolution of stresses in space and is in agreement with the conceptual aspect of this demonstration which is based on a simple point source. Note that our demonstration is done for a tridimensional medium but because $r \gg h$ in practice, only stress evolutions on a horizontal plane will be shown.

[9] Let us consider the following conditions:

$$\begin{cases} \sigma(r \to \infty) = \sigma_f \\ \sigma(r = 0) = \sigma(r = 0, t) \end{cases} \tag{6}$$

which mean that the loading only affects the stress shadow region through time whereas more distant stress is constant, tending to the failure stress σ_f (i.e., background stress region). Using the conditions from (6) in equations (3) and (4), we find

$$\sigma(r, t) = \frac{h^3}{(r^2 + h^2)^{3/2}} \left(\sigma_0 - \sigma_f + \frac{d\sigma_l}{dt} t \right) + \sigma_f \tag{7}$$

Equation (7) gives the evolution at the surface of the stress shadow ($\sigma < 0$) as a function of the distance from the source point (i.e., epicenter) and of the time from the last main shock ($t_0 = 0$) to the next one (t_f) and is shown in Figure 2. Note that except close to the source, the evolution is the same at any depth that is small compared to r.

2.2. Background Stress Noise

[10] We now consider the background stress noise $\Delta\sigma_b$ as follows:

$$\Delta\sigma_b = \sigma_f - \sigma^* \tag{8}$$

where σ^* is approaching σ_f. The peaks of the background stress noise (defined as each different value of σ^* in space) are random uniform in space and amplitude. The background stress noise is considered random to determine the only effects of the spatiotemporal evolution of the stress shadow on accelerating moment release. The use of a more complex but more realistic background stress field would only obscure the result of this demonstration.

[11] Fluctuations of the background stress noise $\Delta\sigma_b$ must be such that the events that result from relaxing stress peaks ($\sigma^* \to \sigma_f$) result in a set of events obeying the Gutenberg-Richter frequency-magnitude relation (Figure 3). The appropriate scaling law can be implemented in various

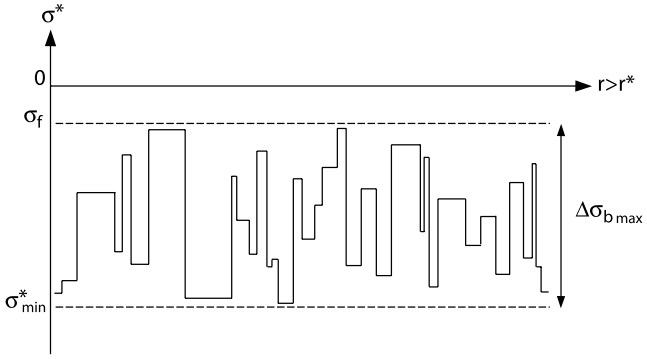

Figure 3. Background stress noise $\Delta\sigma_b$. Stress fluctuations σ^* are approaching the failure stress σ_f. The peaks of the background stress noise (defined as each different value of σ^* in space) are randomly uniform in space and amplitude. The stress distribution is such that the events that result from relaxing stress peaks ($\sigma^* \rightarrow \sigma_f$) result in a set of events obeying the Gutenberg-Richter frequency-magnitude relation, following *King and Bowman* [2003] (see text for details). Note that $r > r^*$ corresponds to a distance from the source point (main shock) where the associated stress shadow has no influence on the background stress.

ways as explained by *King and Bowman* [2003], and the easiest one is to adjust the size of the stress peaks and earthquake magnitude for any irregular function. A simple random stress distribution σ^* can be created by assigning random numbers to each element of a matrix. All points of the matrix that equal or exceed the failure stress σ_f are associated with an earthquake. The areas A of these regions are calculated to provide a measure of events size. These areas are then scaled such that the resulting value is equivalent to an earthquake of magnitude M ($M = A^s$, with s a scaling parameter which depends of the range of areas A and of the range of magnitudes M chosen). With the appropriate scaling coefficients, this provides a Gutenberg-Richter relation with a b value of 1.

[12] We then define the region of background stress as the region where the stress shadow has no influence, at $r > r^*$. Also, we define a constant background stress noise that corresponds to the maximum amplitude $\sigma_f - \sigma^*_{\min}$. In the following demonstration, we will consider the stress noise $\Delta\sigma_b$ constant.

2.3. Decrease of the Size of the Stress Shadow

[13] We define the following conditions:

$$\begin{cases} \sigma(r^*, t) = \sigma^* \\ \sigma(r = 0, t_f) = \sigma_f \end{cases} \tag{9}$$

The first condition from (9) means that the spatial limit of the stress shadow is at r^* when the stress σ is indistinguishable from the background stress σ^*.

[14] Then using conditions from (9) in equation (7), we find

$$\begin{cases} \frac{h^3}{\left(r^{*2}+h^2\right)^{3/2}}\left(\sigma_0 - \sigma_f + \frac{d\sigma_l}{dt}t\right) + \sigma_f = \sigma^* \\ \sigma_0 + \frac{d\sigma_l}{dt}t_f = \sigma_f \end{cases} \tag{10}$$

By substitution of σ_0, we obtain

$$\frac{h^3}{\left(r^{*2}+h^2\right)^{3/2}}\left(\frac{d\sigma_l}{dt}\left(t_f - t\right)\right) = \Delta\sigma_b \tag{11}$$

which leads to

$$r^*(t) = h\left[\left(\frac{d\sigma_l}{dt}\frac{\left(t_f - t\right)}{\Delta\sigma_b}\right)^{2/3} - 1\right]^{1/2} \tag{12}$$

[15] Equation (12) gives the decrease of the size of the stress shadow as a function of time t from $t = 0$ to t_f and is represented in Figure 4. For a point at a distance from the source point $r < r^*$, it is located in the stress shadow ($\sigma(r, t) < \sigma^*$). For a point at a distance from the source point $r \geq r^*$, it is located outside the stress shadow, in the background stress noise ($\sigma(r, t) = \sigma^*$). It is important to note that the stress shadow does not disappear at the time t_f but at

$$t_{f'} = t_f - \Delta t \quad , \quad \Delta t = \frac{\Delta\sigma_b}{d\sigma_l/dt} \tag{13}$$

when the stress shadow is undistinguishable from the background stress σ^* at $r^* = 0$. Therefore the main shock can occur between $t_{f'}$ and t_f due to the stress noise perturbation (with $t_{f'} < t_f$).

2.4. Time-to-Failure Power Law Equation

[16] We now use equation (12) to describe the evolution of seismicity λ as a function of time t. We first consider the simple form

$$\lambda(t) = c_\lambda A(t) \tag{14}$$

with A the area where events occur as a function of time t and c_λ a constant that corresponds to the density of events per unit area (i.e., background density).

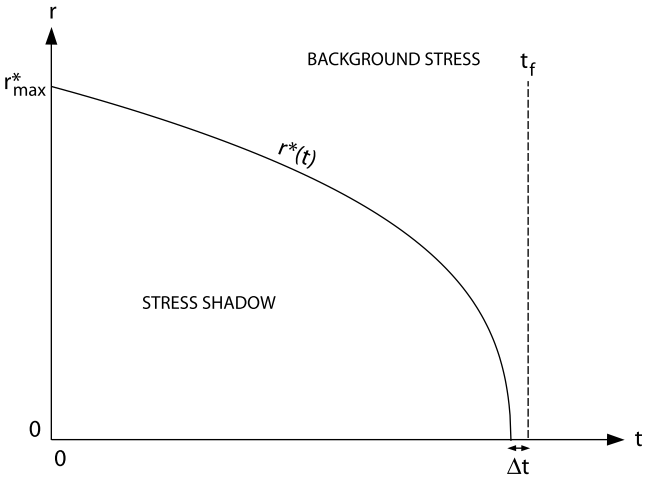

Figure 4. Decrease of the size of the stress shadow r^* as a function of time t from $t = 0$ to t_f. For a point at a distance from the source point $r < r^*$, it is located in the stress shadow ($\sigma(r, t) < \sigma^*$). For a point at a distance from the source point $r \geq r^*$, it is located outside the stress shadow, in the background stress noise ($\sigma(r, t) = \sigma^*$). It is important to note that the stress shadow does not disappear at the main shock time t_f but at $t_f - \Delta t$ (see text for details).

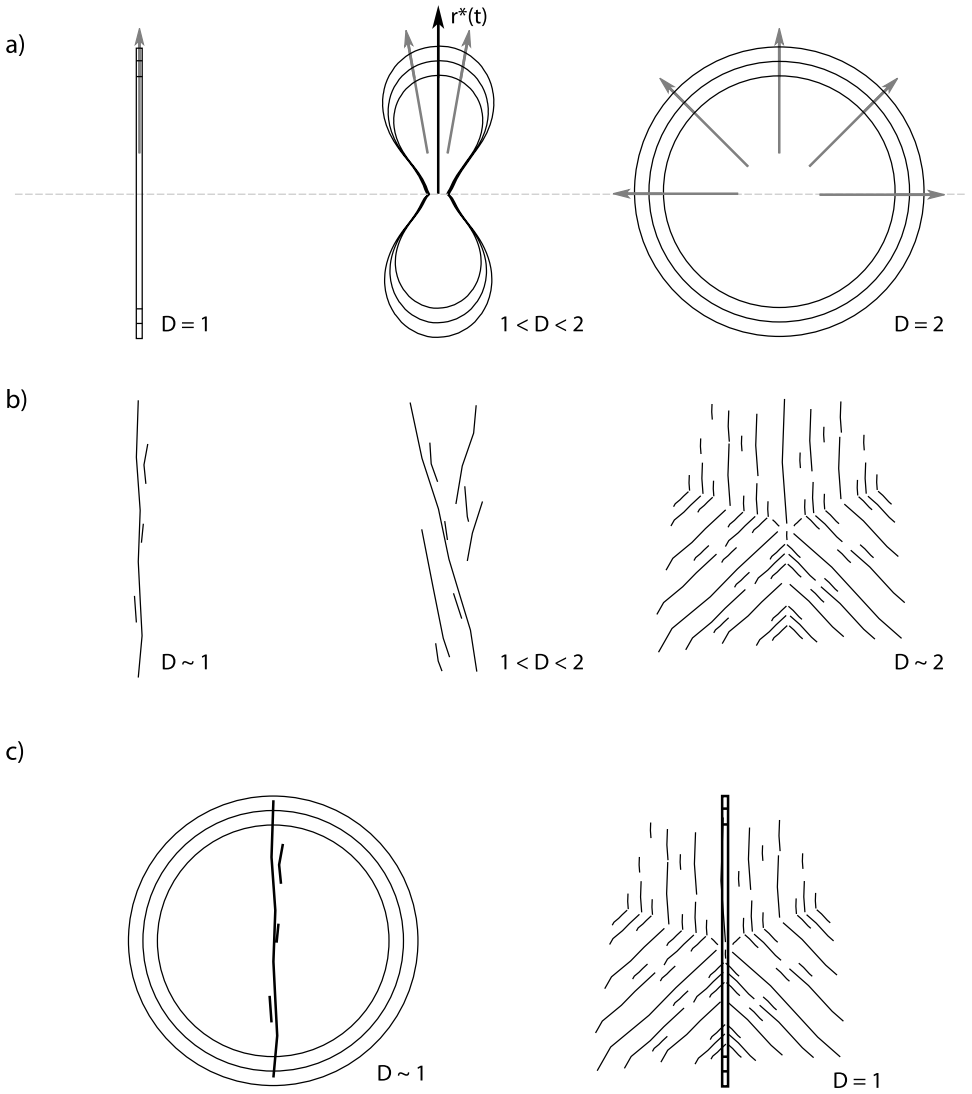

Figure 5. Variability of the parameter D for different geometrical shapes of the stress shadow and for different distributions of active faults. These two criteria must be taken into account to determine the spatial distribution of the theoretical precursory seismicity. (a) Geometrical shape. $D = 1$ for a straight line, $D = 2$ for a circle, and $1 \leq D \leq 2$ for a stress lobe. This can be explained by the fact that a change of the surface of a stress lobe is not homogeneous in all directions of space. Gray arrows show the directions of extension of the geometrical shapes. (b) Fractal dimension of the fault network. $D = 1$ for a straight-line fault, $D = 2$ for a surface completely filled by faults, $1 \leq D \leq 2$ for a surface partially filled by faults. (c) D corresponding to the lowest value from the geometrical shape or from the fractal dimension.

[17] In the stress accumulation model [*King and Bowman*, 2003], accelerating moment release corresponds to events that occur where the stress shadow is filled by loading at depth ($d\sigma_l/dt$). Thus we can define the evolution of accelerating moment release λ_{AMR} through time t as

$$\lambda_{AMR}(t) = c_\lambda[A_{sh}(t_0) - A_{sh}(t)] \quad , \qquad t_0 = 0 \tag{15}$$

with A_{sh} the surface of the stress shadow and $A_{sh}(t_0)$ the initial surface of the stress shadow (when $r = r^*_{\max}$). We can also define the evolution of the background seismicity λ_b where the stress shadow has no influence (where $r \geq r^*$) as

$$\lambda_b(t) = c_\lambda A_b \delta_b t \tag{16}$$

with A_b a predefined surface (minus the stress shadow surface $A_{sh}(t_0)$) and δ_b the background seismicity rate per unit area, assuming that the background seismicity is constant through time.

[18] We now introduce equation (12) in

$$A_{sh}(t) = k_A r^{*D}(t) \tag{17}$$

with k_A a constant that is linked to the geometrical shape of the surface A_{sh} and D the dimension of the geometrical shape. In a simple case where the stress shadow is circular and seismicity uniformly distributed in space, parameters of Equation 17 would be $k_A = \pi$ and $D = 2$. However, the geometrical shape of stress lobes cannot be simply

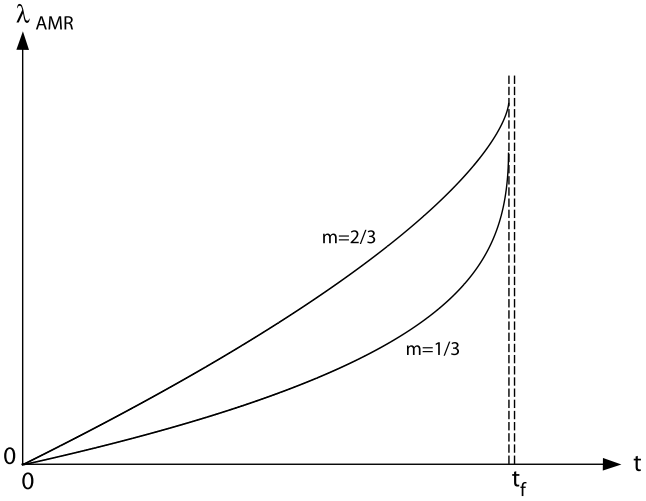

Figure 6. Possible shapes for the time-to-failure power law equation defined from the stress accumulation model. For two-dimensional faulting, $1/3 \leq m \leq 2/3$. Note that the two curves have been rescaled for display reasons.

determined analytically only numerically. Also, seismicity is not uniformly distributed in space but is self-similar due to the fact that events can be associated with fault systems. This must be taken into account in equation (17) since the area A_{sh} is assumed to correspond to the spatial distribution of seismicity. Thus D is linked to the shape of the stress lobes and to the distribution of active faults. For an homogeneous distribution of events, D only depends of the geometrical shape of the stress shadow. By analogy to simple geometrical patterns such as a straight line ($D = 1$) and a circle ($D = 2$), a stress lobe corresponds to $1 \leq D \leq 2$ because a change of its size is not homogeneous in all directions of space (Figure 5a). The spatial distribution of faults can be characterized (in theory at least) by an appropriate spatial fractal. In this case, a fractal generator with a dimension of 1 is equivalent to a straight line, a generator with a dimension of 2 can completely fill an area, and a generator with a dimension of 3 can fill space. For two-dimensional faulting, the surface will be partially filled with $1 \leq D \leq 2$ [e.g., *King*, 1983] (Figure 5b). Thus D corresponds to the lowest value obtained from the geometrical shape or from the fractal dimension of the fault network. For example, if the geometrical shape is a circle, D should be equal to 2 but if seismicity occurs on a fault network of fractal dimension 1, D will be equal to 1 (Figure 5c).

[19] With these geometrical considerations in mind, we can now study the shape of the accelerating moment release time-to-failure equation predicted by the stress accumulation model. From equations (12), (15), and (17), we find

$$\lambda_{AMR} \propto -\left(\frac{d\sigma_l}{dt}\frac{t_f - t}{\Delta\sigma_b}\right)^{D/3}, \quad 1 \leq D \leq 2 \tag{18}$$

[20] By analogy with the accelerating moment release power law time-to-failure equation (1), we obtain

$$\frac{1}{3} \leq m \leq \frac{2}{3} \tag{19}$$

This result is in agreement with m values found for real data (Table 1) and is represented in Figure 6 based on

$$\lambda_{AMR}(t) = c_\lambda k_A h^D \left[\left(\left(\frac{d\sigma_l}{dt}\frac{t_f}{\Delta\sigma_b}\right)^{2/3} - 1\right)^{D/2} - \left(\left(\frac{d\sigma_l}{dt}\frac{t_f - t}{\Delta\sigma_b}\right)^{2/3} - 1\right)^{D/2}\right] \tag{20}$$

which is the complete formulation of Equation 18 that corresponds to the time-to-failure power law equation defined from the stress accumulation model.

3. Discussion

3.1. A Noncritical Origin of the Time-to-Failure Power Law

[21] Other authors have considered that the stress accumulation model [*King and Bowman*, 2003] is a critical point process [e.g., *Sammis and Sornette*, 2002; *Tiampo and Anghel*, 2006]. This is not the case (see below) although the stress accumulation model could be parameterized as a class of percolation critical point models if it is treated as a driven threshold with a mean field approximation [*Sammis and Sornette*, 2002]. However, this does not add to our understanding of the mechanical processes.

[22] The fact that the stress accumulation model is not based on critical processes can be demonstrated by the following arguments:

[23] 1. Loading processes are due to stable sliding at depth during the seismic cycle of a given fault.

[24] 2. The main shock is due to loading processes and not to preevent seismicity, distant from the fault. In other words, the main shock is not the final result of a cascading phenomenon, but the processes originally described by *Reid* [1910] as elastic rebound.

[25] 3. Events that compose accelerating moment release (AMR) are due to loading processes. Whereas aftershocks relax the excess stresses generated by a main shock, AMR events relax excess stresses generated by loading. As a consequence, they delay (slightly) the time of occurrence of the future main shock. This is opposite to the concept of cascade triggering from the smallest events to the largest one.

[26] 4. The Gutenberg-Richter law, often considered as a signature of critical phenomena [e.g., *Bak and Tang*, 1989; *Sornette et al.*, 1990; *Blanter et al.*, 1997], is not a necessary condition for the emergence of a time-to-failure power law pattern.

Table 1. List of m Values Determined From the Study of Accelerating Moment Release in Different Regions

m Value	Region	Reference
0.30 (0.10–0.39)	northern California	*Bufe and Varnes* [1993]
0.26 (0.10–0.55)	California	*Bowman et al.* [1998]
0.24 (0.12–0.47)	New Madrid Seismic Zone	*Brehm and Braile* [1998]
0.47 (0.27–0.70)	Aegean region	*Papazachos and Papazachos* [2000]
0.36 (0.29–0.46)	New Zealand	*Robinson*, 2000]
0.34 (0.29–0.40)	northwest Anatolia	*Papazachos et al.* [2002]

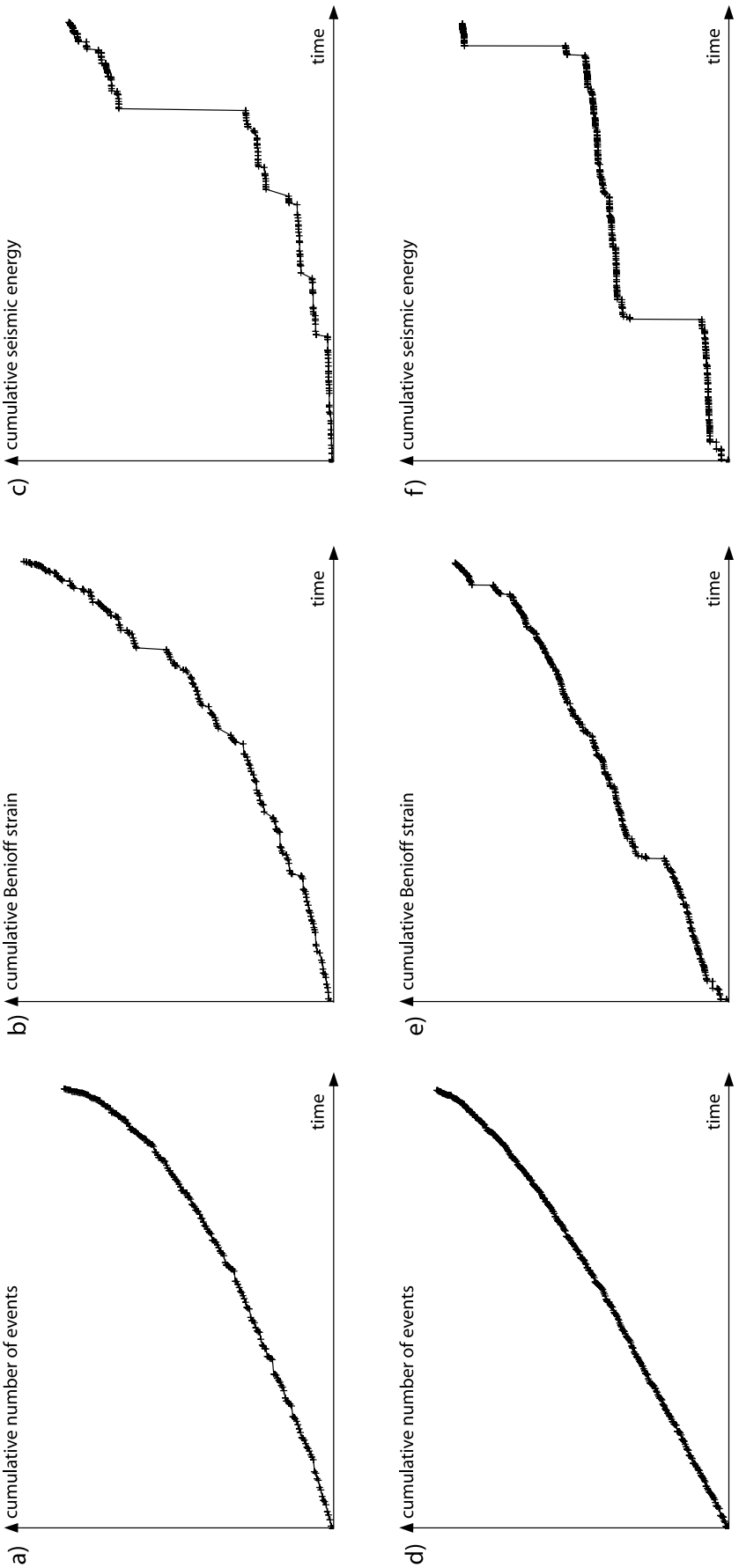

Figure 7. Two examples of seismicity distribution (random uniform in space, random in magnitude in respect to the Gutenberg-Richter law). The first one corresponds to the expected seismicity evolution in the region of accelerating seismicity (power law) following equation (20) (Figures 7a, 7b, and 7c) and the second one corresponds to an association of accelerating seismicity (power law) following equation (20) and of background seismicity (linear law) following equation (16) (Figures 7d, 7e, and 7f). (a and d) Cumulative number of events through time; (b and e) cumulative Benioff strain through time (i.e., accelerating moment release); and (c and f) cumulative seismic energy through time.

[27] In our study, we do not claim that critical processes do not exist. Loading processes (stress accumulation model) and stress triggering (e.g., epidemic-type aftershock sequence model) should be seen as independent processes that may superimpose their effects but stress triggering is not the cause of AMR [*Mignan et al.*, 2006b]. It is also important to note that we do not consider that all critical processes involve cascade triggering. However, other critical models such as percolation models [e.g., *Sammis and Sornette*, 2002], as explained earlier, do not add to our understanding of the mechanical processes. Rupture processes on the fault are commonly considered to be due to critical phenomena [e.g., *Allegre et al.*, 1982], but the stress accumulation model is not concerned with these processes which are therefore not discussed here.

3.2. Acceleration of the Number of Events Versus Accelerating Moment Release

[28] It can be noted that the quantity $\lambda_{AMR}(t)$ corresponds to the evolution of the cumulative number of events through time, whereas accelerating moment release is defined by the evolution of the cumulative Benioff strain through time (equation (1)). However, the choice of the cumulative Benioff strain to fit accelerating seismicity has never been shown to be the most appropriate parameter, only a convenient observational tool (as explained previously).

[29] In the stress accumulation model, the time power law is due to the decrease of the size of the stress shadow which is similar to an increase of the size of the region of background seismicity. By consequence, the studied parameter $\lambda_{AMR}(t)$ is linked to the density of events per unit of space and not to their magnitude. This is in agreement with the fact that accelerating moment release usually corresponds to an increase of the a value and not of the b value [e.g., *Sammis et al.*, 2004].

[30] We now add to equation (20) an appropriate noise to simulate the Gutenberg-Richter statistics to compare the power law time-to-failure equation with real data. Figure 7 shows two examples of seismicity distribution (random uniform in space, random in magnitude in respect to the Gutenberg-Richter law). The first one corresponds to the expected seismicity evolution in the region of accelerating seismicity (power law) following equation (20) (Figures 7a, 7b, and 7c), and the second one corresponds to an association of accelerating seismicity (power law) following equation (20) and of background seismicity (linear law) following equation (16) (Figures 7d, 7e, and 7f). This second example simulates a case where accelerating seismicity is searched in such a way that the optimized region contains events that are part of the acceleration but also some independent events from the background, where $r > r^*_{max}$ (see Figure 4).

[31] Figure 7 also shows the variability of the power law time-to-failure curve for different criteria (cumulative number of events, cumulative Benioff strain and cumulative seismic energy). From our formulation, it is evident that the best acceleration is found for the cumulative number of events (Figure 7a). Acceleration is also clear for the cumulative Benioff strain and accelerating moment release simulated using equation (20) is similar to real patterns (Figure 7b). We can note that no acceleration is visible for the cumulative seismic energy due to the role of the largest events of the fractal noise (Figure 7c). In the case that a linear seismicity contribution is added, depending on the random noise, accelerating moment release can become difficult to observe (Figures 7b and 7e).

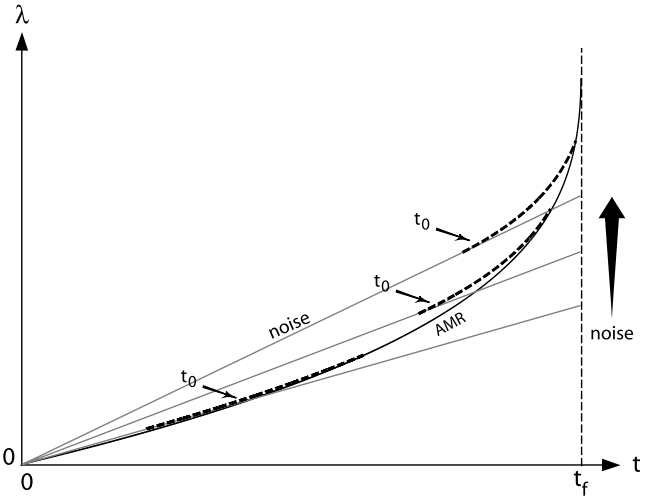

Figure 8. Schematic representation of the observed duration of accelerating precursory seismicity. Accelerating moment release is masked by background noise (constant rate). The greater the noise, the later in the seismic cycle that acceleration is observable; t_0 indicates the approximate starting time determined from a temporal search.

3.3. Duration of Accelerating Seismicity

[32] The mathematical formulation of accelerating seismicity shows that acceleration should be observed throughout the seismic cycle. However, if the signal is perturbed by background noise, the acceleration appears later during the seismic cycle, as observed in simulations by *King and Bowman* [2003] and in real data by *Bowman and Sammis* [2004]. This phenomenon is illustrated schematically in Figure 8 and can explain why no correlation has yet been made between the duration of acceleration moment release and the recurrence time of large earthquakes on a same fault. Because of the power law behavior, the curve is at first undistinguishable from a straight line.

[33] A better determination of the spatial distribution of precursory seismicity, such as done by *Bowman and King* [2001] and *Mignan et al.* [2006b], may permit some background seismicity noise to be removed and to extract accelerating patterns over longer time periods.

4. Conclusion

[34] The mathematical formulation of accelerating seismicity based on the stress accumulation model permits low level regional seismic activity to be related to the loading rate of the fault that is going to fail. Contrary to critical processes, this view links directly the parameters of the acceleration to the behavior of the main fault (loading rate, duration of the seismic cycle). Moreover, it gives a new explanation for the m value which depends on the geometrical shape of the stress shadow and of the fractal dimension of the regional fault network.

[35] The proposed formulation should in the future be used for real data sets, with real fault characteristics, to compare with current time-to-failure analysis employed in earthquake forecasts. The complementary role of the stress accumulation model to the concept of seismic gap and time recurrence of large earthquakes has already been discussed by *Mignan et al.* [2006a], and at present, the loading rate is directly integrated in the power law time-to-failure equation of accelerating moment release. Although at present we do not yet know how well the parameters in the equation can be determined and the degree to which this will improve the identification of AMR, nonetheless having a clear mathematical description of the process is the best approach to improve AMR related seismic hazard determination.

[36] **Acknowledgments.** The authors acknowledge helpful reviews by Charles Sammis and an anonymous reviewer, as well as Associate Editor Steven Cohen. The authors also thank Renata Dmowska for helpful suggestions and critical comments. This research was supported by the INSU-CNRS and the Southern California Earthquake Center. SCEC is funded by NSF Cooperative Agreement EAR-0106924 and USGS Cooperative Agreement 02HQAG0008. This paper is IPGP contribution 2223, INSU contribution 401, and SCEC contribution 1079.

References

Allegre, C. J., J. L. Le Mouel, and A. Provost (1982), Scaling rules in rock fracture and possible implications for earthquake predictions, *Nature*, *297*, 47–49.

Bak, P., and C. Tang (1989), Earthquakes as a self-organized critical phenomenon, *J. Geophys. Res.*, *94*, 15,635–15,637.

Ben-Zion, Y., and V. Lyakhovsky (2002), Accelerated seismic release and related aspects of seismicity patterns on earthquake faults, *Pure Appl. Geophys.*, *159*, 2385–2412.

Blanter, E. M., M. G. Shnirman, and J. L. Le Mouel (1997), Hierarchical model of seismicity: Scaling and predictability, *Phys. Earth Planet. Inter.*, *103*, 135–150.

Bowman, D., and C. G. Sammis (2004), Intermittent criticality and the Gutenberg-Richter distribution, *Pure Appl. Geophys.*, *161*, 1945–1956.

Bowman, D. D., and G. C. P. King (2001), Accelerating seismicity and stress accumulation before large earthquakes, *Geophys. Res. Lett.*, *28*, 4039–4042.

Bowman, D., G. Ouillon, C. Sammis, A. Sornette, and D. Sornette (1998), An observational test of the critical earthquake concept, *J. Geophys. Res.*, *103*, 24,359–24,372.

Brehm, D. J., and L. W. Braile (1998), Intermediate-term earthquake prediction using precursory events in the New Madrid seismic zone, *Bull. Seismol. Soc. Am.*, *88*, 564–580.

Bufe, C. G., and D. J. Varnes (1993), Predictive modeling of the seismic cycle of the greater San Francisco Bay region, *J. Geophys. Res.*, *98*, 9871–9883.

Jaumé, S. C., and L. R. Sykes (1999), Evolving towards a critical point: A review of accelerating seismic moment/energy release prior to large and great earthquakes, *Pure Appl. Geophys.*, *155*, 279–305.

King, G. (1983), The accommodation of large strains in the upper lithosphere of the Earth and other solids by self-similar fault systems: The geometrical origin of b-value, *Pure Appl. Geophys.*, *121*, 761–815.

King, G. C. P., and D. D. Bowman (2003), The evolution of regional seismicity between large earthquakes, *J. Geophys. Res.*, *108*(B2), 2096, doi:10.1029/2001JB000783.

Knopoff, L., T. Levshina, V. Keilis-Borok, and C. Mattoni (1996), Increased long-range intermediate-magnitude earthquake activity prior to strong earthquakes in California, *J. Geophys. Res.*, *101*, 5779–5796.

Mignan, A., G. C. P. King, D. Bowman, R. Lacassin, and R. Dmowska (2006a), Seismic activity in the Sumatra-Java region prior to the December 26, 2004 (M_w = 9.0–9.3) and March 28, 2005 (M_w = 8.7) earthquakes, *Earth Planet. Sci. Lett.*, *244*, 639–654.

Mignan, A., D. D. Bowman, and G. C. P. King (2006b), An observational test of the origin of accelerating moment release before large earthquakes, *J. Geophys. Res.*, *111*, B11304, doi:10.1029/2006JB004374.

Newman, W. I., and S. L. Phoenix (2001), Time-dependent fiber-bundles with local load sharing, *Phys. Rev. E*, *63*, 021507, doi:10.1103/PhysRevE.63.021507.

Papazachos, B., and C. Papazachos (2000), Accelerated preshock deformation of broad regions in the Aegean area, *Pure Appl. Geophys.*, *157*, 1663–1681.

Papazachos, B. C., A. S. Savvaidis, G. F. Karakaisis, and C. B. Papazachos (2002), Precursory accelerating seismic crustal deformation in the Northwestern Anatolia Fault Zone, *Tectonophysics*, *347*, 217–230.

Reid, H. F. (1910), *Report of the State Investigation Commission*, vol. 2, The Mechanics of the Earthquake: The California Earthquake of April 18, 1906, Carnegie Inst., Washington, D. C.

Robinson, R. (2000), A test of the precursory accelerating moment release model on some recent New Zealand earthquakes, *Geophys. J. Int.*, *140*, 568–576.

Saleur, H., C. G. Sammis, and D. Sornette (1996), Discrete scale invariance, complex fractal dimensions, and log-periodic fluctuations in seismicity, *J. Geophys. Res.*, *101*, 17,661–17,678.

Sammis, C. G., and D. Sornette (2002), Positive feedback, memory, and the predictability of earthquakes, *Proc. Natl. Acad. Sci. U.S.A.*, *99*, 2501–2508.

Sammis, C. G., D. D. Bowman, and G. C. P. King (2004), Anomalous seismicity and accelerating moment release preceding the 2001 and 2002 earthquakes in northern Baja California, Mexico, *Pure Appl. Geophys.*, *161*, 2369–2378.

Sornette, D., and A. Helmstetter (2002), Occurrence of finite-time singularities in epidemic models of rupture, earthquakes, and starquakes, *Phys. Rev. Lett.*, *89*(15), 158501.

Sornette, D., and C. Sammis (1995), Complex critical exponents from renormalization group theory of earthquakes: Implications for earthquake predictions, *J. Phys.*, *5*, 607–619.

Sornette, D., A. Sornette, and P. Davy (1990), Structuration of the lithosphere in plate tectonics as a self-organized critical phenomenon, *J. Geophys. Res.*, *95*, 17,353–17,361.

Sykes, L., and S. Jaumé (1990), Seismic activity on neighboring faults as a long-term precursor to large earthquakes in the San Fransisco Bay area, *Nature*, *348*, 595–599.

Tiampo, K. F., and M. Anghel (2006), Introduction to special issue: Critical point theory and space-time pattern formation in precursory seismicity, *Tectonophysics*, *413*, 1–3.

Turcotte, D. L., W. I. Newman, and R. Scherbakov (2003), Micro- and macro-scopic models for rock fracture, *Geophys. J. Int.*, *152*, 718–728.

Voight, B. (1989), A relation to describe rate-dependent material failure, *Science*, *243*, 200–203.

Zoller, G., S. Hainzl, and J. Kurths (2001), Observation of growing correlation length as an indicator for critical point behavior prior to large earthquakes, *J. Geophys. Res.*, *106*, 2167–2176.

D. Bowman, Department of Geological Sciences, California State University, Fullerton, CA 92834-6850, USA.

G. C. P. King, Laboratoire Tectonique, Institut de Physique du Globe de Paris, 4, place Jussieu, F-75252 Paris Cedex 05, France.

A. Mignan, Risk Management Solutions, Peninsular House, 30 Monument Street, London EC3R 8NB, UK. (arnaud.mignan@rms.com)